

# A Study on the Performance of Approximate Riemann Solvers, Integrators, and Parallelization in the Simulation Code Athena++

1 KIAN M. HAYES<sup>1</sup>

2 <sup>1</sup>*Benedictine College*  
3      1020 N 2nd Street  
4      Atchison, KS 66002, USA

## 5 ABSTRACT

6 The performance of various Riemann solvers in the hydrodynamics simulation code Athena++ is  
7 studied and the results of various test problems using these solvers are presented. Results show  
8 that the LLF solver performs the best as far as time to simulation completion, but the respective  
9 simulations show a lack of resolution in the fluid and a lack of structures present in other solvers. We  
10 confirm as proposed in Stone et al. (2020) that the HLLD and HLLC solvers are most suitable for  
11 general simulations involving shocks and other discontinuities in MHD and hydrodynamic problems  
12 respectively.

13 *Keywords:* These are keywords for the paper

## 14 1. INTRODUCTION

15 In this study, we sought to answer the following:

- 16 a What is the exact performance of all Riemann Solvers in Athena++? How do they perform against each other  
17 and which is the best as far as its computational cost and accuracy?
- 18 b How do the time integrators in Athena++ compare against each other? Do they affect accuracy and what is  
19 their computational cost?
- 20 c What is the parallelization performance of Athena++?

## 21 2. FLUID DYNAMICS AND GOVERNING EQUATIONS

22 For the following study, numerical methods are employed to solve equations of fluid dynamics. This section outlines  
23 the governing equations for both hydrodynamics and magneto-hydrodynamics (MHD). The simulation codes make use  
24 of both Euler and Navier-Stokes Equations for inviscid and viscous flow respectively which are later adapted for the  
25 inclusion of electric and magnetic fields for MHD.

### 26 2.1. Euler's Equations

27 The equations for fluid dynamics are partial differential equations in space and time which are solved iteratively in  
28 numerical problems. Namely, for inviscid flow they are Euler's equations. In one dimension, these are written as:

29  $\rho_t + (\rho u)_x = 0 \quad (1)$

30  $(\rho u)_t + (\rho u^2 + p)_x = 0 \quad (2)$

31  $E_t + [u(E + p)]_x = 0 \quad (3)$

32 Where E is the total energy per unit volume written as:

33

$$E = \rho(\frac{1}{2}V^2 + e) \quad (4)$$

34 where V is the specific kinetic energy written as:

35

$$\frac{1}{2}V^2 = \frac{1}{2}V \cdot V = \frac{1}{2}(u^2 + v^2 + w^2) \quad (5)$$

36 and e is the total internal energy of the system.

37 These equations describe the conservation of mass, momentum, and energy in fluid systems. They can be written  
38 more compactly by defining U as a column vector of conserved variables (i.e. variables differentiated with respect to  
39 time) and F as the flux vector (i.e. variables differentiated with respect to space).

40

$$U_t + F(U)_x = 0 \quad (6)$$

41 Where U and F are column vectors written in matrix notation as

42

$$U = \begin{bmatrix} \rho \\ \rho u \\ E \end{bmatrix}, F = \begin{bmatrix} \rho u \\ \rho u^2 + p \\ u(E + p) \end{bmatrix} \quad (7)$$

## 43 2.2. Navier-Stokes Equations

44 The Navier-Stokes (NS) Equations are similar to the Euler equations except they include viscosity and heat conduction  
45 of the fluid much of which is found in Blazek (2001). For this we introduce the flux vectors of convection and  
46 viscosity in  $F_c$  and  $F_v$ . With this in mind, we can combine integral forms of the conservation laws in

47

$$\frac{\partial}{\partial t} \int W d\Omega + \int (F_c - F_v) dS = \int Q d\Omega \quad (8)$$

48 Where W is likened to U in Eq. 7, in that it is a column vector of conserved variables. For the convective fluxes

49

$$F_c = \begin{bmatrix} \rho V \\ \rho u V + n_x p \\ \rho v V + n_y p \\ \rho w V + n_z p \\ \rho H V \end{bmatrix} \quad (9)$$

50 and for the viscous fluxes

51

$$F_v = \begin{bmatrix} 0 \\ n_x \tau_{xx} + n_y \tau_{xy} + n_z \tau_{yx} \\ n_x \tau_{yx} + n_y \tau_{yy} + n_z \tau_{yz} \\ n_x \tau_{zx} + n_y \tau_{zy} + n_z \tau_{zz} \\ n_x \Theta_x + n_y \Theta_y + n_z \Theta_z \end{bmatrix} \quad (10)$$

52 where

53

$$\Theta_x = u \tau_{xx} + v \tau_{xy} + w \tau_{xz} + k \frac{\partial T}{\partial x} \quad (11)$$

54

$$\Theta_y = u \tau_{yx} + v \tau_{yy} + w \tau_{yz} + k \frac{\partial T}{\partial y} \quad (12)$$

55

$$\Theta_z = u \tau_{zx} + v \tau_{zy} + w \tau_{zz} + k \frac{\partial T}{\partial z} \quad (13)$$

56 which describes the work done on the system due to viscosity with  $\tau$  being the stress tensor. Lastly, we have

**Figure 1.** A graphical representation of the Riemann Problem

$$Q = \begin{bmatrix} 0 \\ \rho f_{e,x} \\ \rho f_{e,y} \\ \rho f_{e,z} \\ \rho f_e \cdot v + \dot{q}_h \end{bmatrix} \quad (14)$$

### 2.3. Conservation Laws in Magneto-Hydrodynamics

For ideal magneto-hydrodynamics (MHD), the conservative equations are written as

$$\frac{\partial \rho}{\partial t} + \nabla \cdot (\rho \mathbf{v}) = 0 \quad (15)$$

$$\frac{\partial \rho \mathbf{v}}{\partial t} + \nabla \cdot (\rho \mathbf{v} \mathbf{v} - \mathbf{B} \mathbf{B}) + \nabla P^* = 0 \quad (16)$$

$$\frac{\partial \mathbf{B}}{\partial t} + \nabla \cdot (\mathbf{v} \mathbf{B} - \mathbf{B} \mathbf{v}) = 0 \quad (17)$$

$$\frac{\partial E}{\partial t} + \nabla \cdot ((E + P^*) \mathbf{v} - \mathbf{B}(\mathbf{B} \cdot \mathbf{v})) = 0 \quad (18)$$

Where  $P^*$  is a diagonal tensor for gas pressure with components  $P^* = P + B^2/2$ ,  $E$  is the energy density, also written as

$$E = \frac{P}{\gamma - 1} + \frac{1}{2} \rho v^2 + \frac{B^2}{2} \quad (19)$$

, and  $B^2 = \mathbf{B} \cdot \mathbf{B}$ . The governing equations above often don't have analytical solutions which begs for the use of computational methods. There are a number of numerical methods to solve these equations for various dynamical systems but a common framework utilized in modern codes including Athena++ MAYBE INCLUDE OTHER CODES is known as the Godunov scheme. The following section outlines this numerical scheme and how it is employed in Athena++.

## 3. THE GODUNOV SCHEME AND RIEMANN PROBLEM

The Godunov Scheme, first proposed by Sergei K. Godunov in 1959 ([Godunov & Bohachevsky 1959](#)), is the numerical scheme utilized in many modern simulation codes including Athena++ that iteratively solves the governing equations in Section 2. INCLUDE WHAT THIS SCHEME IS WITHOUT MENTIONING RIEMANN PROBLEM. Due to the discrete nature of numerical methods, a discontinuity occurs at each cell interface. The problem is an initial boundary value problem and has the basis.

$$\begin{aligned} \text{PDE: } & U_t + F(U)_x = 0 \\ \text{Initial Value: } & U(x, 0) = U^{(0)}(x) \\ \text{Boundary Value: } & U(0, t) = U_1(t), U(L, t) = U_r(t) \end{aligned} \quad (20)$$

Which can be represented graphically in Figure (FIGURE FOR RIEMANN PROBLEMS).

It is required that  $F_{i+1/2}$  be known for the Godunov method but this discontinuity at every interface has non-trivial solutions. This problem is known as a Riemann problem and is a central calculation in the Godunov scheme. There are many methods to solve this problem which are described in the following section, much of which can be found extensively in [Toro \(2009\)](#).

#### 4. RIEMANN SOLVERS

To find the flux at cell interfaces in the Godunov scheme, the use of a Riemann solver is necessary. There are numerous algorithms that solve this problem which make different approximations in order to find a solution. In this section, the different solvers utilized in this study are described.

##### 4.1. HLL and HLLC

The HLL solver was one of the initial algorithm for solving the Riemann Problem, introduced in [Harten et al. \(1983\)](#). The basic formulation of the HLL solver is finding  $F_{i+1/2}$  (as described in [Section 3](#)) by utilizing the left and right wave speeds to approximate the state of the column vector  $U^{hll}$  at the interface. The structure of this solution can be found in [Figure SHOW THE FIGURE WITH THE TWO LINES AND THE SOLUTION BEING BETWEEN THE TWO](#). The state at the interface is said to be between the left and right states, but all solutions are brought together to approximate  $U^{hll}$  which is then used to solve for  $F_{i+1/2}$  using

$$F^{hll} = F_L + S_L(U^{hll} - U_L) \quad (21)$$

or

$$F^{hll} = F_r + S_R(U^{hll} - U_R) \quad (22)$$

We can combine these two equations by applying Rankine–Hugoniot conditions across the left and right waves respectively to get

$$F^{hll} = \frac{S_R F_L - S_L F_R + S_L S_R (U_R - U_L)}{S_R - S_L} \quad (23)$$

Using this, The intercell flux  $F_{i+\frac{1}{2}}^{hll}$  then can be written as

$$F_{i+\frac{1}{2}}^{hll} = \begin{cases} F_L & 0 \leq S_L \\ \frac{S_R F_L - S_L F_R + S_L S_R (U_R - U_L)}{S_R - S_L} & S_L \leq 0 \leq S_R \\ F_R & 0 \leq S_R \end{cases} \quad (24)$$

Where the intercell flux solution is determined conditionally by the wave speed of the left and right cells. This equation for flux can then employed to complete the Godonuv method. Although, this method is more common to be a basis for others, as it is not effective at solving situations with certain discontinuities which are important in modeling fluid. Such a discontinuity is known as an intermediate wave and is accounted for in the HLLC scheme where the missing middle waves are reincorporated into the structure of the solution of the Riemann problem.

The HLLC involves the similar approximations as stated previously, but now the intermediate wave speed denoted as  $S_*$  is incorporated with the  $S_R$  and  $S_L$  waves. A representation of this is found in [Figure \(FIGURE SHOWING THE STAR REGION GRAPH\)](#). The flux is defined conditionally

$$F_{i+\frac{1}{2}}^{hllc} = \begin{cases} F_L & 0 \leq S_L \\ F_{*L} & S_L \leq 0 \leq S_* \\ F_{*R} & S_* \leq 0 \leq S_R \\ F_R & 0 \leq S_R \end{cases} \quad (25)$$

##### 4.2. HLLE

[\(Einfeldt 1988\)](#)

##### 4.3. HLLD

[\(Miyoshi & Kusano 2005\)](#)

119            4.4. *LHLLD/LHLLC*

120            4.5. *Roe*

121       Originally proposed in (Roe 1981), the Roe method was one of the first attempts to solve the Riemann problem  
 122       algorithmically. The method makes use of a linearized equation in order to find a solution for the flux at the cell  
 123       interface  $F_{i+1/2}$ . It has gone many iterations since its first introduction but here the original approach by Roe will be  
 124       outlined. Roe solves the Riemann problem by introducing the Jacobian Matrix denoted as

$$125 \quad A(U) = \frac{\partial F}{\partial U} \quad (26)$$

126       Which allows for 6 to be written as

$$127 \quad U_t + A(U)U_x = 0 \quad (27)$$

128       in which Roe replaces the matrix  $A(U)$  with a constant one

$$129 \quad \tilde{A} = \tilde{A}(U_L, U_R) \quad (28)$$

130       This allows for (27) to be written in a linear form with

$$131 \quad U_t + \tilde{A}U_x = 0 \quad (29)$$

$$132 \quad U(x, 0) = \begin{cases} U_L, & x \leq 0 \\ U_R, & x \geq 0 \end{cases}$$

133       This is now simply an eigenvalue-eigenvector equation in which solving for the eigenvalues  $\tilde{\lambda}_i$  of the Jacobian matrix  
 134        $\tilde{A}$  allows for the Riemann problem to be solved exactly with

$$135 \quad F_{i+1/2} = \frac{1}{2}(F_L + F_R) - \frac{1}{2} \sum_{i=1}^m \tilde{\alpha}_i |\tilde{\lambda}_i| \tilde{K}^{(i)} \quad (30)$$

136       where  $m$ ,  $\tilde{\alpha}_i$ ,  $\tilde{\lambda}_i$ , and  $\tilde{K}^{(i)}$  are respectively the number of conservation laws to be solved, wave strength, the eigenvalues  
 137       of  $\tilde{A}$ , and the right eigenvectors. The method for obtaining these values is outlined further in Toro (2009).

138            4.6. *LLF*

139            5. DESCRIPTION OF TESTS PROBLEMS

140       The test problems employed by this test include two hydrodynamic tests and one MHD test. Namely, the Lecoanet  
 141       Kelvin-Helmholtz Instability (Lecoanet et al. 2016), Liska & Wendroff Implosion (Liska & Wendroff 2003), and MHD  
 142       Spherical Blast (Gardiner & Stone 2005). These were chosen to fully study the hydrodynamic and MHD capabilities  
 143       of Athena++ and their scalability. To make a problem more or less computationally intensive is a matter of changing  
 144       the simulation time, boundary size, or number of cells. All of which can be edited easily in the respective Athena  
 145       input file. These problems also serve as standard tests for fluid discontinuities in most simulation codes.

146            5.1. *Rayleigh-Taylor Instability*

147            5.2. *Implosion*

148       The second hydro test problem used in this study is the 2D implosion test as outlined in Liska & Wendroff (2003).  
 149       The main feature of this problem is a fluid with a diamond-shaped interface at the center of the boundaries with a  
 150       density  $\rho_i$  and a separate density  $\rho_e$  surrounded by this inner density. The effect of this initial condition is a collapse  
 151       of the fluid toward the center of the box, causing an implosion. The test in this study is of the variation as seen in  
 152       Stone et al. (2020) where the first quadrant of the aforementioned box is the boundary rather than the full diamond  
 153       as seen in the original paper. A graphical representation of this setup can be found in FIGURE FOR THE INITIAL  
 154       SET-UP OF IMPLOSION TEST.

### 5.3. Lecoanet Kelvin-Helmholtz Instability

The Kelvin-Helmholtz Instability is a common test problem in fluid simulation codes as it provides the conditions for testing highly discontinuous systems. This instability occurs at the interface between high and low density in fluid and is a common phenomenon across the universe. This includes meteorology, atmospheres, aeronautics, stellar systems, and protoplanetary disks. The instability has a cascading effect in fluids making it a prominent source of mixing and turbulence. The particular variation of this instability used in this study is one described in [Lecoanet et al. \(2016\)](#) which has the following initial conditions:

$$\begin{aligned}
\rho &= 1 + \frac{\Delta\rho}{\rho_0} \left( \frac{1}{2} \tanh\left(\frac{z-z_1}{a}\right) - \tanh\left(\frac{z-z_2}{a}\right) \right) \\
u_x &= u_{\text{flow}} \left( \tanh\left(\frac{z-z_1}{a}\right) - \tanh\left(\frac{z-z_2}{a}\right) - 1 \right) \\
u_z &= A \sin(2\pi x) \left( \exp\left(-\frac{(z-z_1)^2}{\sigma^2}\right) + \exp\left(-\frac{(z-z_2)^2}{\sigma^2}\right) \right) \\
P &= P_0 \\
c &= \frac{1}{2} \left( \tanh\left(\frac{z-z_2}{a}\right) - \tanh\left(\frac{z-z_1}{a}\right) + 2 \right)
\end{aligned} \tag{31}$$

Respective constants reflect that which is found in Lecoanet et al. (2016) with  $a = 0.05$ ,  $\sigma = 0.2$ ,  $u_{flow} = 1$ , and  $P_0 = 10$  so that the flow is subsonic with a Mach number  $M \approx 0.25$  in regions with  $\rho = 1$  and  $M \approx 0.35$  in regions with  $\rho = 2$ . Lastly, the amplitude of the initial velocity perturbation is  $A = 0.01$ . The specific runtime parameters for the simulations ran specifically in this study can be found in the Results section (i.e. simulation time, limits, and mesh grid deconstruction).

#### 5.4. MHD Blast

the MHD test problem conducted in this study is the MHD Blast problem as found in [Gardiner & Stone \(2005\)](#). It considers the explosion of a centrally over-pressurized region into a low-pressure, low ambient medium.

## 6. NUMERICAL METHOD, ATHENA++

Athena ++ (Stone et al. 2020) is an open-source simulation code built for solving the governing equations of fluid dynamics in the Godonuv scheme using SMR/AMR and comes with a suite of test problems including those described in the above section. It was chosen for its ease of use and widely available support for the various for the topics studied in this paper.

## 7. RESULTS

### 7.1. Solvers Test

## 7.2. Integrators Test

### 7.3. Parallelization Test

## 8. CONCLUSION

#### Acknowledgments for the paper

*Software:* yt Project for visualizations (Turk et al. 2011), Athena++ (Stone et al. 2020). The GitHub repository containing the Python and Bash scripts to conduct this study along with simulation videos for the various test problems can be found at <https://github.com/kianhayes/summer2024>.

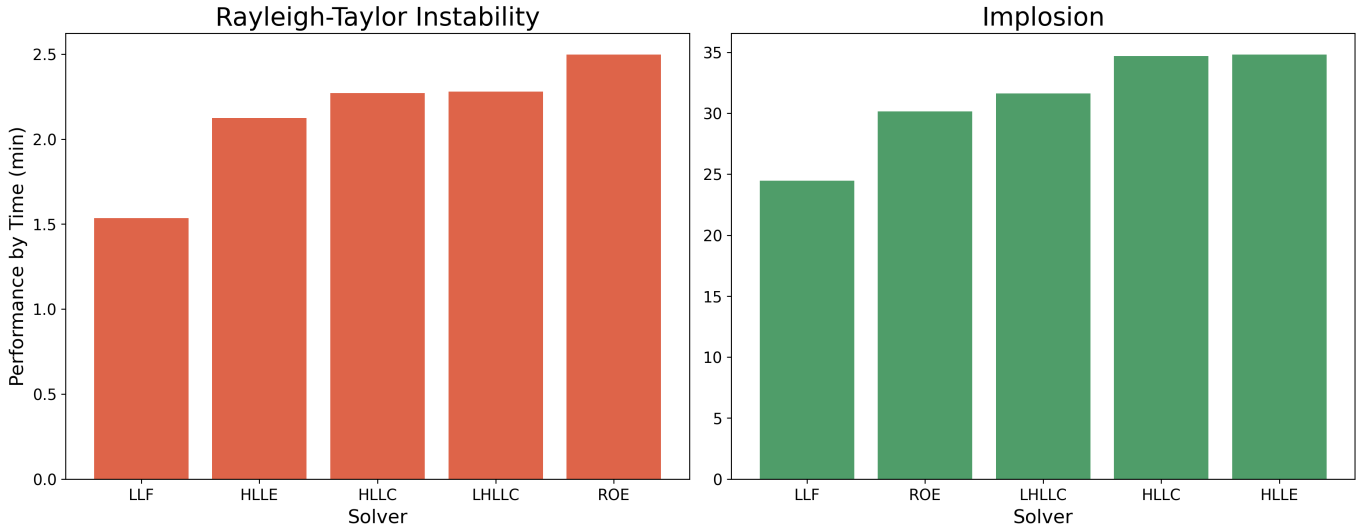


**Figure 2.** RAYLEIGH Taylor is spelled wrong

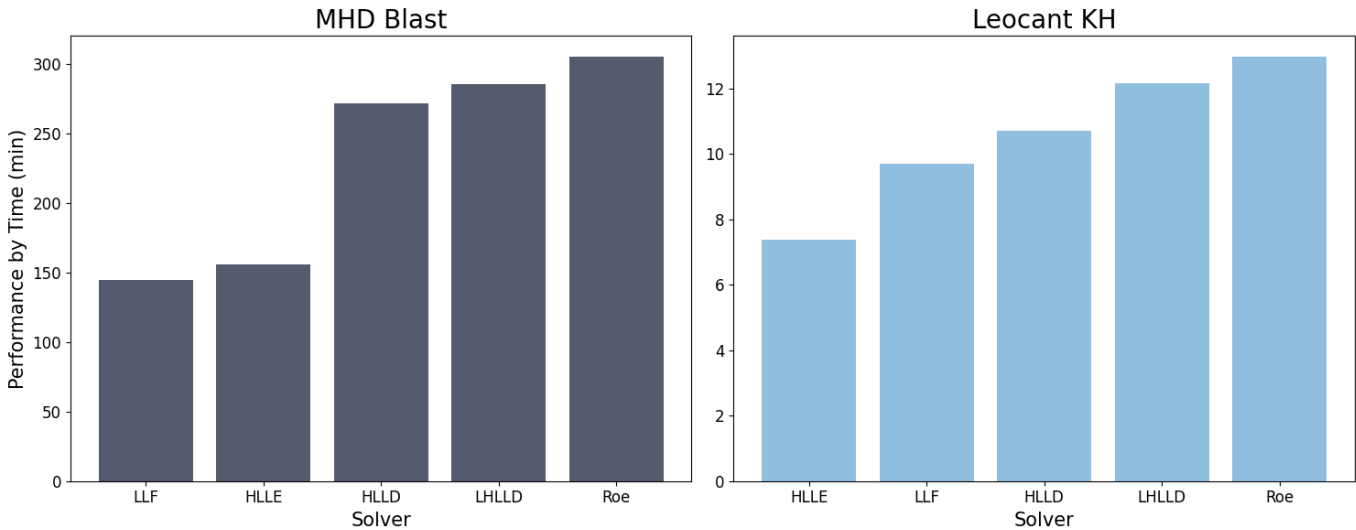


**Figure 3.** Caption

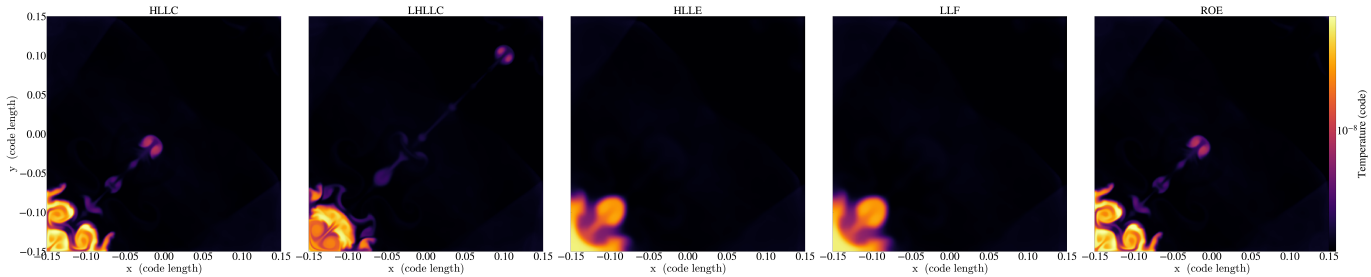


**Figure 4.** Caption

## REFERENCES

- 190 Blazek, J. 2001, Computational Fluid Dynamics: Principles 193 Einfeldt, B. 1988, SIAM Journal on Numerical Analysis, 25,  
191 and Applications (Elsevier Science). 194 294, doi: [10.1137/0725021](https://doi.org/10.1137/0725021)  
192 <https://books.google.com/books?id=asWGy362QFIC>

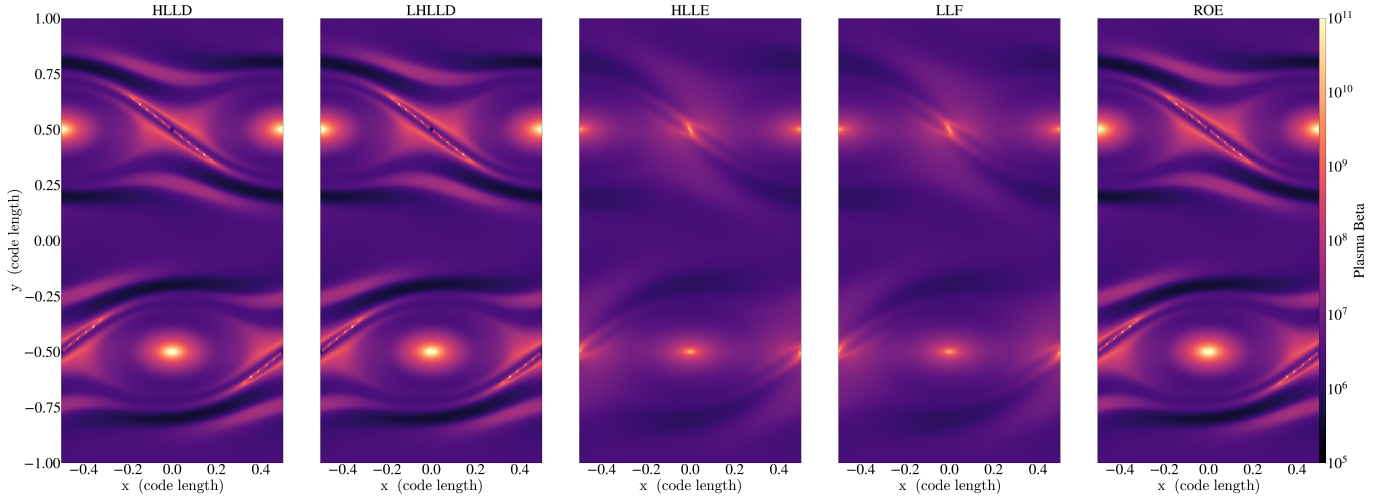


**Figure 5.** Caption

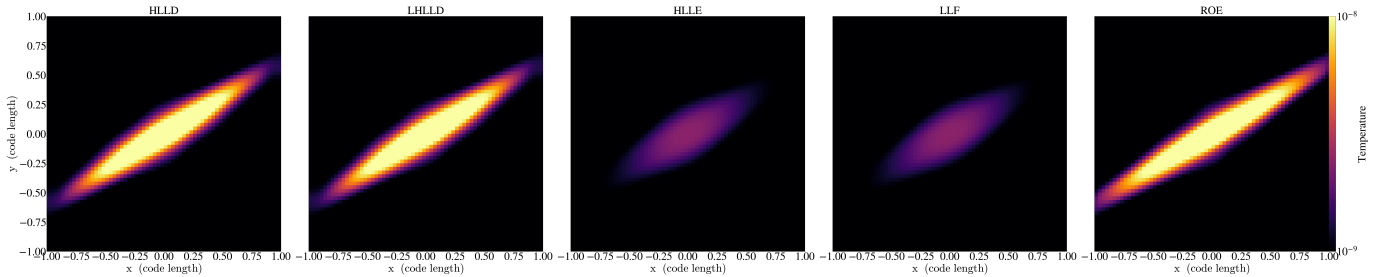


**Figure 6.** Caption

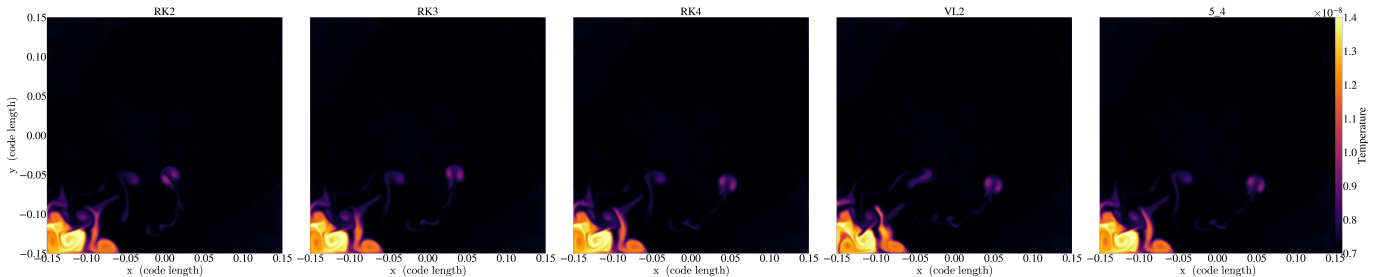


**Figure 7.** Caption

- 195 Gardiner, T. A., & Stone, J. M. 2005, Journal of  
196 Computational Physics, 205, 509,  
197 doi: [10.1016/j.jcp.2004.11.016](https://doi.org/10.1016/j.jcp.2004.11.016)
- 198 Godunov, S. K., & Bohachevsky, I. 1959, Matematicheskij  
199 sbornik, 47(89), 271. <https://hal.science/hal-01620642>
- 200 Harten, A., Lax, P., & van Leer, B. 1983, SIAM Rev, 25, 35
- 201 Lecoanet, D., McCourt, M., Quataert, E., et al. 2016,  
202 Monthly Notices of the Royal Astronomical Society, 455,  
203 4274, doi: [10.1093/mnras/stv2564](https://doi.org/10.1093/mnras/stv2564)
- 204 Liska, R., & Wendroff, B. 2003, SIAM Journal on Scientific  
205 Computing, 25, 995, doi: [10.1137/S1064827502402120](https://doi.org/10.1137/S1064827502402120)
- 206 Miyoshi, T., & Kusano, K. 2005, Journal of Computational  
207 Physics, 208, 315,  
208 doi: <https://doi.org/10.1016/j.jcp.2005.02.017>
- 209 Roe, P. 1981, Journal of Computational Physics, 43, 357,  
210 doi: [https://doi.org/10.1016/0021-9991\(81\)90128-5](https://doi.org/10.1016/0021-9991(81)90128-5)
- 211 Stone, J. M., Tomida, K., White, C. J., & Felker, K. G.  
212 2020, ApJS, 249, 4, doi: [10.3847/1538-4365/ab929b](https://doi.org/10.3847/1538-4365/ab929b)
- 213 Toro, E. F. 2009, Riemann Solvers and Numerical Methods  
214 for Fluid Dynamics: A Practical Introduction (Berlin,  
215 Heidelberg: Springer), doi: [10.1007/b79761](https://doi.org/10.1007/b79761)
- 216 Turk, M. J., Smith, B. D., Oishi, J. S., et al. 2011, ApJS,  
217 192, 9, doi: [10.1088/0067-0049/192/1/9](https://doi.org/10.1088/0067-0049/192/1/9)

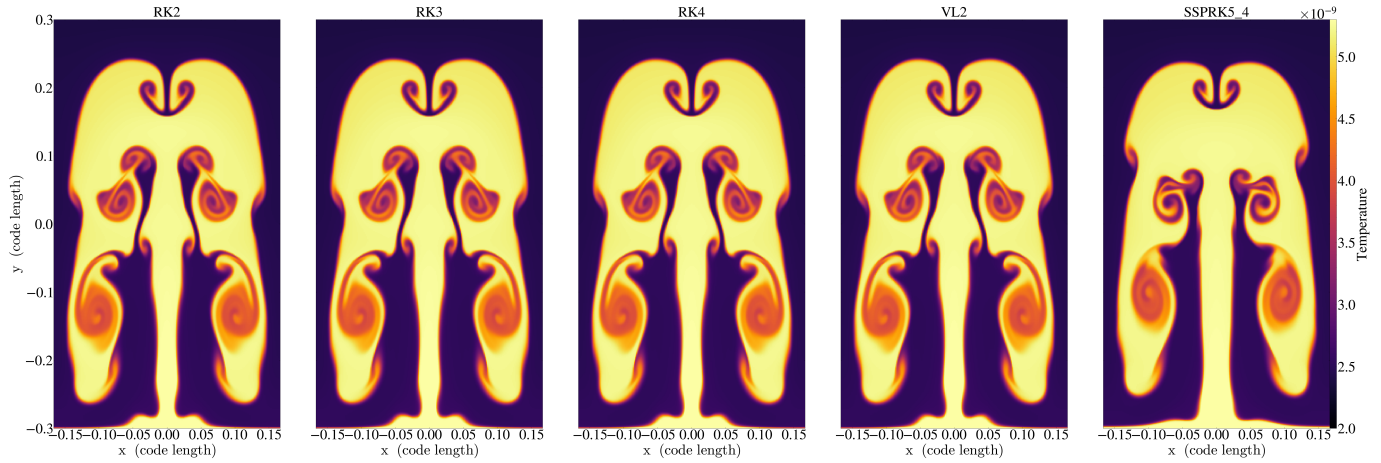


**Figure 8.** Caption

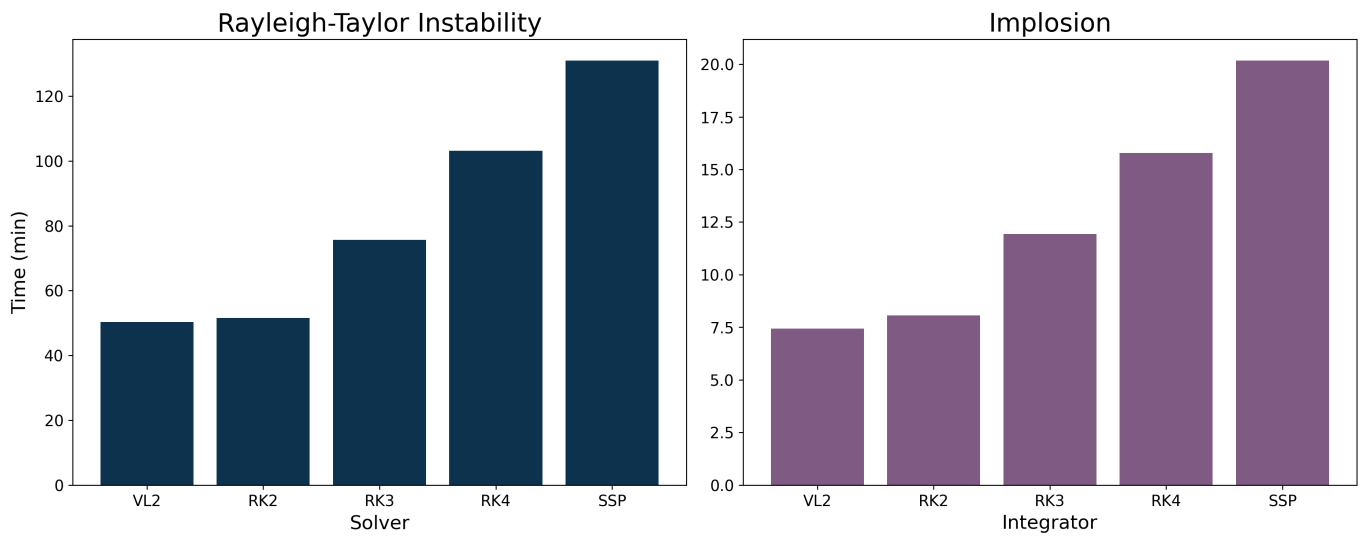


**Figure 9.** Caption

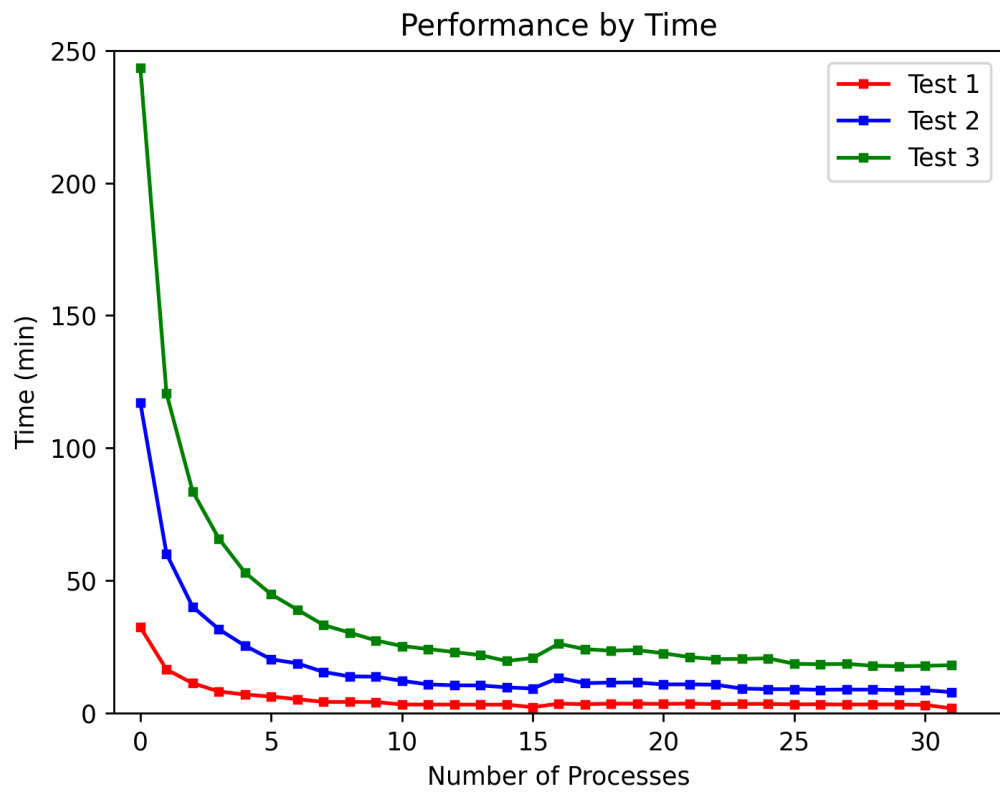


**Figure 10.** Caption